Composite Solid Polymer Electrolytes Based on Pluronics: Does Ordering Matter?

Lyudmila M. Bronstein,*[,†] Robert L. Karlinsey,[§] Zheng Yi,[‡] John Carini,[‡] Ulli Werner-Zwanziger,[||] Peter V. Konarev,[⊥,#] Dmitri I. Svergun,[⊥,#] Angelica Sanchez,[▽] and Saad Khan[▽]

Departments of Chemistry and Physics, Indiana University, Bloomington, Indiana 47405; Indiana Nanotech, Indianapolis, Indiana 46202; Department of Chemistry and Institute for Research in Materials, Dalhousie University, Halifax NS B3H 4J3, Canada; EMBL, Hamburg Outstation, Notkestrasse 85, D-22603 Hamburg, Germany; Institute of Crystallography, Russian Academy of Sciences, Leninsky pr. 59, 117333 Moscow, Russia; and Department of Chemical and Biomolecular Engineering, North Carolina State University, Raleigh, North Carolina 27695

Received August 7, 2007. Revised Manuscript Received October 5, 2007

Composite solids polymer electrolytes (SPEs) based on Pluronic block copolymers, PEO_x-*b*-PPO_y-*b*-PEO_x, and silicate organic–inorganic component (OIC) formed in situ have been synthesized and characterized using solid-state NMR, Raman spectroscopy, differential scanning calorimetry (DSC), small-angle X-ray scattering (SAXS), rheology, and electrochemical measurements. Raman spectroscopy, DSC, and rheological data reveal that the block copolymer and OIC are intermixed in the composite SPEs, and the degree of intermixing determines the SPE properties. Comparison of the SAXS and electrochemical results leads us to conclude that ordering in block copolymer-based composite SPEs is not a crucial parameter for the improved conductivity, while the combination of the ratios of the SPE components and their intermixing gives rise to extended interfaces that control the electrochemical performance.

1. Introduction

One of the modern trends in development of solid polymer electrolytes (SPEs) based on "salt-in-polymer" (normally poly(ethylene oxide) {PEO} + Li salt) systems is strengthening the material either through cross-linking[1,2] or by incorporating an inorganic component.[1,3–25] Several advantages can be expected from introduction of an inorganic component. While the primary advantage of introducing an inorganic component is the increased strength of the polymer composite, other benefits include the possibility to influence the degree of crystallinity of the PEO, by changing conditions for polymer chain arrangement, and the electrochemical properties of the SPEs. Recently, a new family of organic–inorganic composites (OICs) which includes mesoporous aluminosilicate[26–29] or silicate[30] with attached polyether chains has been developed. The attached polyether chains

* To whom correspondence should be addressed. E-mail: lybronst@indiana.edu.
† Department of Chemistry, Indiana University.
‡ Department of Physics, Indiana University.
§ Indiana Nanotech.
|| Dalhousie University.
⊥ EMBL.
Russian Academy of Sciences.
▽ North Carolina State University.

(1) Meyer, W. H. *Adv. Mater.* **1998**, *10*, 439.
(2) Zhang, Z.; Lyons, L. J.; Amine, K.; West, R. *Macromolecules* **2005**, *38*, 5714.
(3) Giannelis, E. P. *Adv. Mater.* **1996**, *8*, 29.
(4) Croce, F.; Appetecchi, G. B.; Persi, L.; Scrosati, B. *Nature (London)* **1998**, *394*, 456.
(5) Appetecchi, G. B.; Croce, F.; Persi, L.; Ronci, F.; Scrosati, B. *Electrochim. Acta* **2000**, *45*, 1481.
(6) Lemmon, J. P.; Wu, J.; Oriakhi, C.; Lerner, M. M. *Electrochim. Acta* **1995**, *40*, 2245.
(7) Kurian, M.; Galvin, M. E.; Trapa, P. E.; Sadoway, D. R.; Mayes, A. M. *Electrochim. Acta* **2005**, *50*, 2125.
(8) Hutchison, J. C.; Bissessur, R.; Shriver, D. F. *Chem. Mater.* **1996**, *8*, 1597.
(9) Scrosati, B. *Nature (London)* **1995**, *373*, 557.
(10) Nookala, M.; Kumar, B.; Rodrigues, S. *J. Power Sources* **2002**, *111*, 165.
(11) Wang, C.; Xia, Y.; Koumoto, K.; Sakai, T. *J. Electrochem. Soc.* **2002**, *149*, A967.
(12) Persi, L.; Croce, F.; Scrosati, B.; Plichta, E.; Hendrickson, M. A. *J. Electrochem. Soc.* **2002**, *149*, A212.
(13) Li, Q.; Imanishi, N.; Takeda, Y.; Hirano, A.; Yamamoto, O. *Ionics* **2002**, *8*, 79.
(14) Digar, M.; Hung, S.-L.; Wen, T.-C. *J. Appl. Polym. Sci.* **2001**, *80*, 1319.
(15) Wieczorek, W.; Lipka, P.; Zukowska, G.; Wycislik, H. *J. Phys. Chem. B* **1998**, *102*, 6968.
(16) Best, A. S.; Adebahr, J.; Jacobsson, P.; MacFarlane, D. R.; Forsyth, M. *Macromolecules* **2001**, *34*, 4549.
(17) Marcinek, M.; Bac, A.; Lipka, P.; Zalewska, A.; Zukowska, G.; Borkowska, R.; Wieczorek, W. *J. Phys. Chem. B* **2000**, *104*, 11088.
(18) Adebahr, J.; Best, A. S.; Byrne, N.; Jacobsson, P.; MacFarlane, D. R.; Forsyth, M. *Phys. Chem. Chem. Phys.* **2003**, *5*, 720.
(19) Cheung, I. W.; Chin, K. B.; Greene, E. R.; Smart, M. C.; Abbrent, S.; Greenbaum, S. G.; Prakash, G. K. S.; Surampudi, S. *Electrochim. Acta* **2003**, *48*, 2149.
(20) Sadoway, D. R.; Huang, B. Y.; Trapa, P. E.; Soo, P. P.; Bannerjee, P.; Mayes, A. M. *J. Power Sources* **2001**, *621*, 97–98.
(21) Soo, P. P.; Huang, B. Y.; Jang, Y. I.; Chiang, Y. M.; Sadoway, D. R.; Mayes, A. M. *J. Electrochem. Soc.* **1999**, *146*, 32.
(22) Capiglia, C.; Mustarelli, P.; Quartarone, E.; Tomasi, C.; Magistris, A. *Solid State Ionics* **1999**, *118*, 73.
(23) Kumar, B.; Rodrigues, S. J.; Scanlon, L. G. *J. Electrochem. Soc.* **2001**, *148*, A1191.
(24) Morita, M.; Fujisaki, T.; Yoshimoto, N.; Ishikawa, M. *Electrochim. Acta* **2001**, *46*, 1565.
(25) Sun, H. Y.; Sohn, H.-J.; Yamamoto, O.; Takeda, Y.; Imanishi, N. *J. Electrochem. Soc.* **1999**, *146*, 1672.
(26) Ulrich, R.; Zwanziger, J. W.; De Paul, S. M.; Richert, R.; Wiesner, U.; Spiess, H. W. *Polym. Mater. Sci. Eng.* **1999**, *80*, 610.
(27) Templin, M.; Wiesner, U.; Spies, H. W. *Adv. Mater.* **1997**, *9*, 814.
(28) Bronstein, L. M.; Joo, C.; Karlinsey, R.; Ryder, A.; Zwanziger, J. W. *Chem. Mater.* **2001**, *13*, 3678.

10.1021/cm7022218 CCC: $37.00
Published on Web 11/15/2007

Table 1. Composition, Thermal Properties, and Conductivities of SPEs Based on Silicate OIC and Block Copolymers[a]

Pluronic notation	block copolymer structure	sample notation	T_g, °C	T_m, °C	ΔH,[b] J/g	σ,[c] S/cm
L64	PEO_{13}-*b*-PPO_{31}-*b*-PEO_{13}	Pl-L64-SiO_2/Al	−55 (−67)[d]	no peak (20)	no peak (23.0)	2.3×10^{5}
F68	PEO_{75}-*b*-PPO_{31}-*b*-PEO_{75}	Pl-F68-SiO_2/Al	−43 (−63)	35 (51)	0.42 (87.3)	4.6×10^{-5}
F88	PEO_{109}-*b*-PPO_{41}-*b*-PEO_{109}	Pl-F88-SiO_2/Al	−40 (−65)	41 (57)	0.49 (92.5)	3.0×10^{-5}
F108	PEO_{136}-*b*-PPO_{52}-*b*-PEO_{136}	Pl-F108-SiO_2/Al	−41 (−66)	42 (55)	0.67 (99.5)	2.5×10^{-5}
	PEO_{14} (600 MW)	PEG600-SiO_2/Al	−57			2.8×10^{-5}

[a] Amount of inorganic precursor in SPEs is 55% (calculated toward the PEO phase only). [b] ΔH is the specific enthalpy. [c] σ is the conductivity at room temperature. [d] For T_g, T_m, and ΔH, the numbers in parentheses are for the corresponding block copolymer.

make this composite intimately compatible with PEO, while the inorganic component provides a stabilizing structure.[31,32] In a previous work we characterized the structure, mobility, and conductivity of such hybrid SPEs and the effects of these properties on PEO molecular weight, material composition, and some other parameters.[28–30,33] In this study we elucidate the influence of the polymeric component structure and ordering on the properties of composite SPEs.

Previously, we reported composite SPEs where PEO was replaced with low molecular weight block copolymers such as polystyrene-*block*-poly(ethylene oxide) (PS_{10}-*b*-PEO_{23}) and polyethylene-*block*-poly(ethylene oxide) (PE_{16}-*b*-PEO_{41}).[34] In the case of PS_{10}-*b*-PEO_{23}, the PEO phase of the composite SPE displayed higher glass transition temperature (T_g) than that of the SPEs based on analogous PEO homopolymer and also reduced conductivity. For the PE_{16}-*b*-PEO_{41}, both T_g and conductivity slightly increased, but the latter still did not exceed 10^{-5} S/cm. We believe that the mediocre properties of the SPEs based on PS_{10}-*b*-PEO_{23} are due to the low mobility of the PS block. We found that the T_g of very short PS blocks is still above room temperature,[35] which affects the mobility of the PEO blocks. Soo et al. showed that when both blocks of phase-separated block copolymer are in the rubbery state (T_gs are well below room temperature), these materials exhibit improved conductivities over those of glassy–rubbery block copolymer systems.[21] Indeed, in PE_{16}-*b*-PEO_{41} with both blocks having low T_g values (according to ref 36 the T_g of amorphous PE is −128 °C), the mobility is not impeded, leading to higher conductivity.[34] The small-angle X-ray scattering (SAXS) examination of this SPE showed that the system is mainly disordered; the lack of ordering was attributed to a comparatively short hydrophobic and hydrophilic blocks.

Kao et al.[37] recently reported improved electrochemical properties of composite polymer electrolytes based on Pluronic F127 (PEO_{105}-*b*-PPO_{70}-*b*-PEO_{105}, M_w = 12 600, BASF) and silicate for [O]/[Li] = 16. They suggested that block copolymer ordering allows enhanced conductivity (3.17×10^{-5} S/cm), while for disordered composites at [O]/[Li] = 32 and [O]/[Li] = 8, the conductivities are much lower.[37]

In order to better understand the effects of ordering of Pluronic-based composites on their electrochemical properties, we synthesized hybrid composite SPEs based on Pluronics (PEO_n-*b*-PPO_m-*b*-PEO_n) of different compositions at [O]/[Li] = 14, which was found to be the optimal ratio for these particular systems.[28,38] The OIC is composed of tetramethoxysilane (TMOS) to form a stable tridimensional structure, (3-glycidylpropyl)trimethoxysilane (GLYMO) to provide good miscibility with PEO-containing block copolymer, and 0.65 mol % Al(tri-*sec*-butoxide) (AB) to ensure full polymerization of the GLYMO glycidyl groups and chemical stability of the SPEs synthesized. Here we report on synthesis and properties of these SPE systems using solid-state NMR, Raman spectroscopy, differential scanning calorimetry (DSC), small-angle X-ray scattering (SAXS), rheology, and electrochemical measurements. In particular, we investigate the effect of the SPE ordering on their electrochemical properties.

2. Experimental Part

2.1. Materials. Poly(ethylene glycol) (PEG) with a molecular weight of 600 Da was purchased from Aldrich and used as received. The Pluronics L64, F68, F88, and F108 (Table 1) were obtained from BASF and used without purification. Li triflate (LiTf), tetrahydrofuran (THF), aluminum(tri-*sec*-butoxide) (AB), tetramethoxysilane (TMOS) (Aldrich), chloroform (EM Ind., Inc.), and (3-glycidylpropyl)trimethoxysilane (GLYMO, Fluka) were used without further purification. Water was purified with a "Barnstead NANOpure water" purification system.

2.2. Synthesis. Synthesis of the organic–inorganic composite SPEs based on block copolymers and silicate OIC was carried out by a procedure published elsewhere.[30] In a typical experiment, 0.5 g (9 mmol of PEO) of F108 in 5 mL of chloroform was mixed with 0.1.g (0.64 mmol) of Li triflate in 5 mL of THF. After 30 min stirring, the solution was set aside. The inorganic part of the composite was prepared by a sol–gel reaction of a mixture of GLYMO with TMOS in a molar ratio of 80:20 with addition of a catalytic amount of AB. For this, the weighed vial with a stir bar was charged with 2.66 g (11.25 mmol) of GLYMO, 0.426 g (2.81 mmol) of TMOS, and 0.02 g (0.08 mmol) of AB. The hydrolysis

(29) Bronstein, L. M.; Karlinsey, R. L.; Ritter, K.; Joo, C.-G.; Stein, B.; Zwanziger, J. W. *J. Mater. Chem.* **2004**, *14*, 1812.
(30) Bronstein, L. M.; Karlinsey, R.; Stein, B.; Zwanziger, J. W. *Solid State Ionics* **2005**, *176*, 559.
(31) Templin, M.; Franck, A.; Du Chesne, A.; Leist, H.; Zhang, Y.; Ulrich, R.; Schadler, V.; Wiesner, U. *Science* **1997**, *278*, 1795.
(32) De Paul, S. M.; Zwanziger, J. W.; Ulrich, R.; Wiesner, U.; Spiess, H. W. *J. Am. Chem. Soc.* **1999**, *121*, 5727.
(33) Bronstein, L. M.; Karlinsey, R. L.; Stein, B.; Yi, Z.; Carini, J.; Zwanziger, J. W. *Chem. Mater.* **2006**, *18*, 708.
(34) Bronstein, L. M.; Karlinsey, R.; Ryder, A.; Joo, C.-G.; Zwanziger, J. W. *Polym. Mater. Sci. Eng.* **2001**, *85*, 615.
(35) Bronstein, L. M.; Khotina, I. A.; Chernyshov, D. M.; Valetsky, P. M.; Timofeeva, G. I.; Dubrovina, L. V.; Stein, B.; Karlinsey, R.; Triolo, A.; Weidenmann, A.; Lo Celso, F.; Triolo, R.; Khokhlov, A. R. *J. Colloid Interface Sci.* **2006**, *299*, 944.
(36) Cowie, J. M. G.; McEwen, I. J. *Macromolecules* **1977**, *10*, 1124.
(37) Kao, H.-M.; Chen, C.-L. *Angew. Chem., Int. Ed.* **2004**, *43*, 980.
(38) Ulrich, R.; Zwanziger, J. W.; De Paul, S. M.; Reiche, A.; Leuninger, H.; Spies, H. W.; Wiesner, U. *Adv. Mater.* **2002**, *14*, 1134.

was initiated by adding 15% of equimolar amount (0.12 mL) of water containing HCl (0.01 M solution). After 30 min stirring at room temperature, the reaction mixture was charged with the residue of the 0.01 M HCl solution (0.64 mL) and stirred for 40 min. Then the reaction temperature was raised to 50 °C, the vial was opened, and stirring continued for 15 min. After weighing the vial, the calculated amount of the precondensed silicate sol was added to the solution containing block copolymer and Li salt and stirred for 1 h. The added amount (0.452 g) was determined as 55 wt % OIC in SPE. The reaction solution was spun (or cast) on a Teflon dish and heated at 60 °C for 2 h to allow for solvent evaporation and OIC condensation. The solid film was treated at 130 °C in vacuum for 1 h to complete condensation. Films were easily removed from the dish and ready for examination. Samples were sealed and kept in a desiccator. As shown in ref 28, weight loss from apparent water (up to 150 °C) did not exceed 0.5%.

2.3. Characterization. Differential scanning calorimetry (DSC) was performed using a Q10 TA calorimeter operating in low-temperature mode with liquid nitrogen as the coolant. The samples consisting of 5–12 mg were hermetically sealed in aluminum pans. Dynamic heating scans between −100 and +150 °C at a rate of 10 °C/min were run under a nitrogen atmosphere. Glass transition regions were then determined using the fictive temperature method.[39] Indium and cyclohexane were used as reference standards.

Raman spectra were acquired on a Renishaw RM2000 Raman microscope using a 785 nm diode laser for excitation. The Raman spectra were averaged from several scans. A total acquisition time from 30 min to 1 h was used.

Solid-state ^{13}C and ^{29}Si NMR spectra were acquired on a Bruker DSX Avance spectrometer using a 9.4 T magnet, magic angle spinning (MAS), and cross-polarization (CP) from protons. The ^{13}C CP/MAS NMR spectra were recorded using rotors of 4 mm diameter and spinning up to 11 kHz. The ^{29}Si CP/MAS NMR experiments were performed using rotors of 7 mm diameter. The spinning speeds were varied up to 6.00 kHz to distinguish spinning sidebands from the center band.

Ac impedance spectroscopy was used to measure conductivity and dielectric constants of cast films. To obtain excellent electrode–electrolyte contact, gold electrodes of a known area (0.0647 cm^2) were directly attached to the film by sputter-coating, using a Polaron E5100 sputter-coater. Films were then placed in a home-built temperature-controlled cell for measurements using a HP 4192A impedance analyzer and a Quantum Design digital RG bridge (model 1802, to measure and control the cell temperature). The admittance response of the material was measured in two ways. At a fixed or controlled temperature, data were collected by sweeping the frequencies from 5 Hz to 10 MHz with a 1 V signal (to improve the response from thick films). Bulk conductances were then extrapolated by modeling the admittance of the sample at medium to high frequencies. Alternately, during continuous heating, cooling, or annealing runs, the frequency was kept fixed at 50 kHz, and the conductance value at that frequency was used as the bulk value. (This agrees within 20% of the value obtained from modeling the frequency response.) Both silicon and $(PEO)_{14}LiO_3SCF_3$ were used as reference materials for conductivity. Dielectric constants were obtained by taking the minimum in a capacitance versus frequency curve. Pure PEO ($\epsilon_r \sim 5$)[40] was used as a reference material.

Variable temperature (VT) conductivity measurements were carried out using the following protocol. First, room temperature conductivity of the sample was measured using the HP impedance analyzer. Then the sample was cooled to −50 °C while continuously measuring the sample admittance at 50 kHz. After that the sample was heated in 10 deg steps back to room temperature, measuring the ac admittance from 5 Hz to 10 MHz at −50, −40, . . ., 20 °C. Then the sample was heated from room temperature to 80 °C in 10 deg steps, measuring the ac admittance from 5 Hz to 10 MHz at 30, 40, . . ., 80 °C. At this point the conductivity is in a nearly "as delivered" state from −50 to 80 °C. The sample was held at 80 °C for several hours while measuring the sample admittance at 50 kHz continuously (until the conductivity stops decreasing). Then the sample was cooled back to room temperature, and the sample admittance at 50 kHz was measured continuously. Finally, the sample was held for 4 days at room temperature and conductivity was measured.

The rheology experiments were performed in a stress-controlled rheometer, TA AR2000 at 25 °C, using an 8 mm parallel plate geometry. The procedure employed to make and load the samples was as follows. The samples were cut into 8 mm diameter disks with a razor blade. Each disk was handled with tweezers at all times. The disks were loaded in the rheometer, and the plates were brought together until the normal force indicated 2–3 N. The samples were solidlike, and no relaxation occurred before starting the experiments; thus, the results reported here were run under this compression condition.

The stress sweeps were done at 1 rad/s between 10 and 10^6 Pa, and the frequency sweeps were run between 0.1 and 100 rad/s. In the frequency sweep experiments, the wave shape was always sinusoidal, indicating that neither wall slip nor nonlinear behavior was observed.

The synchrotron radiation X-ray scattering (SAXS) data were collected on the X33 beamline of the EMBL at the storage ring DORIS III (DESY, Hamburg, Germany).[41] The data were recorded using two linear multiwire proportional gas detectors, at the sample–detector distances of 2.4 and 1.0 m and a wavelength $\lambda = 0.15$ nm, covering range of momentum transfer $0.13 < s < 3.3$ nm^{-1} for the first detector and $2.5 < s < 9.0$ nm^{-1} for the second detector ($s = 4\pi \sin\theta/\lambda$, where 2θ is the scattering angle). The powder samples (SPE films were ground with mortar and pestle) were loaded into a silver cell with mica windows, a cell volume of 100 μL, and an optical path length of 1 mm. The measurements were done at room temperature. The focusing geometry and narrow wavelength band-pass ($\Delta\lambda/\lambda \approx 0.005$) resulted in negligible smearing effects. To check for radiation damage, the data were collected in five successive 1 min frames; no radiation effects were observed. The data were averaged after normalization to the intensity of the incident beam and corrected for the detector response. All data manipulations were performed using the program package PRIMUS.[42] The structural parameters were estimated using program PEAK.[42] The long-range order dimension (L) estimating the size of the quasi-crystalline zones in the samples and the degree of disorder in the system ($\Delta/\bar{d}$) were determined from the following expressions:[43]

$$L = \frac{\lambda}{\beta_s \cos\theta} \tag{1}$$

$$\Delta/\bar{d} = \frac{1}{\pi}\sqrt{\frac{\beta_s \bar{d}}{\lambda}} \tag{2}$$

where β_s is the full width at half-maximum intensity of the peak (in radians) observed at a mean scattering angle of 2θ, $\bar{d} = 2\pi/s_{max}$

(39) Schawe, J. E. K. *J. Polym. Sci., Part B* **1998**, *36*, 2165.
(40) McCrum, N. G.; Read, B. E.; Williams, G. *Inelastic and Dielectric Effects in Polymeric Solids*; Dover: New York, 1967.
(41) Boulin, C. J.; Kempf, R.; Gabriel, A.; Koch, M. H. J. *Nucl. Instrum. Methods* **1988**, *269*, 312.
(42) Konarev, P. V.; Petoukhov, M. V.; Volkov, V. V.; Svergun, D. I. *J. Appl. Crystallogr.* **2006**, *39*, 277.
(43) Vainshtein, B. K. *Diffraction of X-rays by Chain Molecules*; Elsevier Publishing Co.: Amsterdam, 1966.

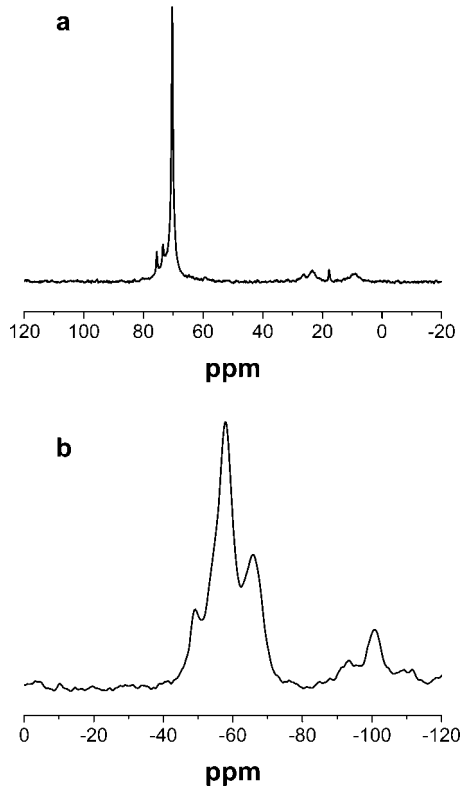

Figure 1. ^{13}C (a) and ^{29}Si (b) CP MAS NMR spectra of F108-SiO_2/Al.

is the characteristic size (periodicity or spacing) of the diffracting structure corresponding to the peak position s_{max}, and Δ is the mean-square deviation of the distance between neighboring layers.

3. Results and Discussion

3.1. Local Structure by NMR. The local structure of the composite SPEs was studied with ^{13}C and ^{29}Si CP/MAS NMR. The carbon and silicon spectra are shown in Figure 1 for a representative material F108-SiO_2/Al, based on Pluronic F108. Other materials show similar spectra. The carbon spectrum shows major resonances, assigned to the CH group of PPO at 75.5 ppm, the –CH_2–O– linkages of PPO (73.5 ppm) and PEO (70.4 ppm) groups,[44] –CH_2– groups of reacted GLYMO (26.1 and 23.4 ppm), the CH_3 group of PPO (17.8 ppm), and –C–Si– units (9 ppm).[28] The absence of two signals at 44 and 51 ppm characteristic of the glycidyl group of GLYMO suggests that this group fully reacts during the SPE formation.[27]

The ^{29}Si CP MAS NMR spectrum contains six signals: T^1 {C–SiO$(OH)_2$}, T^2 {C–SiO_2(OH)}, T^3 {C–SiO_3}, Q^2 {$SiO_3(OH)_2$}, Q^3{SiO_3(OH)}, and Q^4 {SiO_4}. The T^2 and Q^3 species prevail, illustrating a significant but incomplete degree of cross-linking.[30]

3.2. Structure and Mobility by Raman Spectroscopy. In Figure 2 plots are shown for each of the Pluronic-based SPEs on increasing in block copolymer length from bottom to top. The frequency range shown describes the vibrational contributions arising from multiple sources including silica,[45]

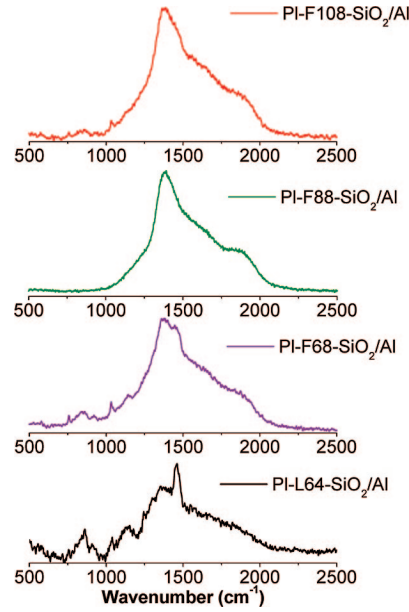

Figure 2. Raman spectra of the SPEs based on L64, F68, F88, and F108 Pluronics.

CF_3SO_3 ions,[46–48] and the PEO-*b*-PPO-*b*-PEO triblock copolymer.[48,49] In the figure, there are distinct vibrations centered near 850 cm^{-1} in the L64, F68, and F108 polymeric systems. These vibrations are most likely due to constrained Si–O–Si bending of the silica component of the composite electrolyte. Additionally, sharp vibrations are clearly observed near 1033 cm^{-1} for these same systems and correspond to the (SO_3) symmetric stretch of the unassociated triflate ion. Surprisingly, these vibrations are not observed in the SPE based on F88, and currently we cannot explain this difference. Near 1140 cm^{-1}, broader signals are observed particularly well in the L64 and F68 polymer systems: in this area the signal likely arises from a combination of Si–O stretching and C–O stretching from components in the triblock copolymer. Based on the nature of the triblock copolymers listed in Table 1, the L64 system manifests the shortest PEO chain in this series and smallest molecular weight. Therefore, it may be likely that more extensive silica clusters are able to nucleate and grow, thus resulting in clearly visible vibrational bands around 850 and 1140 cm^{-1}. Since the character of these vibrations is not well-defined for the other polymer systems, it is likely that the silica component is significantly intermixed (interfaced) with the triblock copolymer. Above 1140 and below 1300 cm^{-1}, contributions from CF_3 and SO_3 stretching of the triflate ion, as well as CH_2 twisting along the triblock copolymer chain, are likely to dominate the vibrational spectra. But the main vibrational events centered near 1370 and 1460 cm^{-1} most likely arise solely from the CH_2 wagging and scissoring from the triblock copolymer. The fact that the triblock copolymer and inorganic fraction of the electrolyte are intermixed gives rise to the broader contribution extending beyond 1500 cm^{-1}

(44) Ma, J.; Guo, C.; Tang, Y.; Wang, J.; Zheng, L.; Liang, X.; Chen, S.; Liu, H. *J. Colloid Interface Sci.* **2006**, *299*, 953.
(45) Walrafen, G. E.; Hokmabadi, M. S.; Holmes, N. C.; Nellis, W. J.; Henning, S. *J. Chem. Phys.* **1985**, *82*, 2472.
(46) Johnston, D. H.; Shriver, D. F. *Inorg. Chem.* **1993**, *32*, 1045.
(47) Girish Kumar, G.; Sampath, S. *Solid State Ionics* **2005**, *176*, 773.
(48) Silva, R. A.; Goulart Silva, G.; Pimenta, M. A. *J. Raman Spectrosc.* **2001**, *32*, 369.
(49) Guo, C.; Liu, H.; Wang, J.; Chen, J. *J. Colloid Interface Sci.* **1999**, *209*, 368.

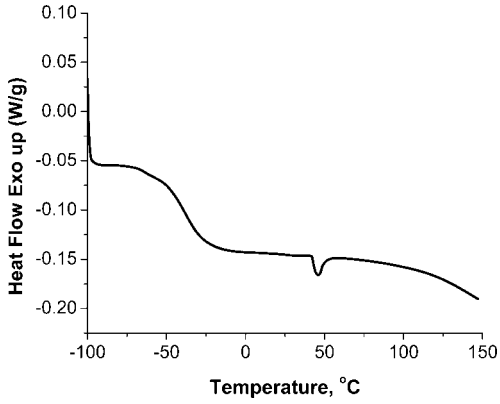

Figure 3. DSC trace of Pl-F108-SiO_2/Al under heating.

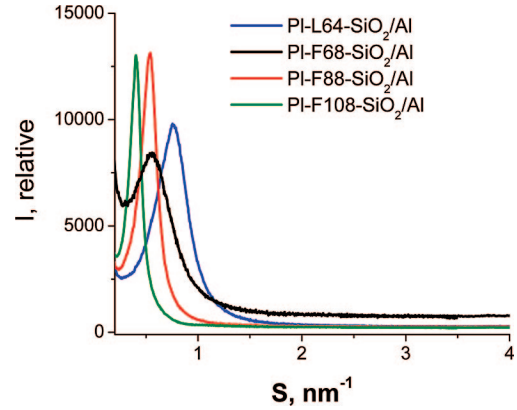

Figure 4. SAXS profiles of the SPEs based on Pluronics with different block length.

to about 2000 cm^{-1}. These high-energy vibrations suggest the methyl wagging along the triblock copolymer chain is constrained heavily by the inorganic component. The SPE based on the shortest triblock copolymer system, L64, does not reveal relatively prominent vibrational shoulders within this vibrational range relative to the SPEs based on larger triblock copolymers. Additionally, the clear distinction of the 1460 cm^{-1} CH_2 scissoring suggests the entire triblock copolymer retains a significant level of flexibility although the growth of additional CH_2 peaks at increased chain lengths both above and below 1460 cm^{-1}, however, suggests the constraints of the composite electrolyte system.

3.3. Polymer Mobility by DSC. To estimate mobility of the polymer chains and their crystallization in the constrained environment of the composite SPEs, we carried out calorimetry measurements (Table 1). It is well established that PEO-*b*-PPO-*b*-PEO block copolymers show only one transition about −70 °C, but this temperature can be lower depending on the block length.[50] From Table 1 one can see that the glass transition temperatures of all composite SPEs are higher than those of the corresponding block copolymer precursors, suggesting a decrease of mobility due to attachment of block copolymer chains to silicate particles.[30,51] Needless to say, the lowest T_g (highest mobility) is observed for the SPE based on L64 block copolymer with the shortest blocks. These data corroborate the Raman spectroscopy data.

A representative DSC trace (for Pl-F108-SiO_2/Al) is presented in Figure 3. The traces of other SPEs look similar except the one for Pl-L64-SiO_2/Al where no melting event is observed. This is not surprising because this SPE is based on the shortest block copolymer whose DSC trace shows the lowest fraction of a crystalline phase. In all other samples the crystallinity is decreased by at least 2 orders of magnitude (judging by the specific enthalpy of melting), indicating that the silicate network largely disrupts the PEO crystallization.

3.4. Room Temperature Conductivity. From Table 1 one can see that conductivity values for all the samples except Pl-F68-SiO_2/Al are nearly the same (2×10^{-5}–3×10^{-5} S/cm) and inconsistent with T_g or crystallinity changes. The highest conductivity (4.6×10^{-5} S/cm) at room temperature is achieved for Pl-F68-SiO_2/Al. This was surprising considering that the polymer mobility here is lower than that of Pl-L64-SiO_2/Al, and some (remnant) crystallinity is present. We think that the highest conductivity of Pl-F68-SiO_2/Al is due to an optimal balance of polymer mobility and interconnectivity with the silicate network.

Table 2. SAXS Structural Parameters of the SPEs Based on Pluronics[a]

sample notation	*L*, nm	*d*, nm	Δ/*d*
Pl-L64-SiO_2/Al	32.3	8.1	0.159
Pl-F68-SiO_2/Al	42.6	10.6	0.159
Pl-F88-SiO_2/Al	45.6	10.9	0.156
Pl-F108-SiO_2/Al	93.3	15.1	0.128

[a] *L* is the long-range order, *d* is the Bragg spacing, and Δ/*d* is the degree of disorder.

3.5. Structure by SAXS. Ordering in the SPEs based on Pluronics was characterized using SAXS. The structural parameters obtained from SAXS patterns (Figure 4) are presented in Table 2. As follows from the SAXS data presented in Figure 4 and Table 2, increase of block length of the PEO-*b*-PPO-*b*-PEO block copolymers results in a larger short-range period (*d*), which is consistent with the increase of the block copolymer size. One can also see a trend of the increase of long-range order, suggesting larger size of ordered areas for larger block copolymers. The higher degree of ordering (Δ/*d*) is observed for the Pl-F108-SiO_2/Al system based on the block copolymer with the highest molecular weight while other systems are mostly disordered. A system is considered poorly ordered at a $\Delta/\bar{d}$ value of 0.15. (as a point of reference, the Bragg peaks nearly disappear when $\Delta/\bar{d} > 0.25$).[43]

Following the conclusions of ref 37 and assuming that the higher ordering should lead to higher conductivity, we tried to increase the degree of ordering in the ordered Pl-F108-SiO_2/Al system by annealing at 60 °C (above melting of crystalline phase)[52] or in the THF (solvent) atmosphere.[53,54] The data presented in Figure 5 illustrate that the heating for 5 h at 60 °C did not influence the type or degree of block copolymer ordering. Similar results were obtained for the

(50) Van Der Schuur, M.; Gaymans, R. J. *J. Polym. Sci., Part A* **2006**, *44*, 4769.
(51) Maitra, P.; Wunder, S. L. *Chem. Mater.* **2002**, *14*, 4494.
(52) Zhang, Y.; Wiesner, U.; Yang, Y.; Pakula, T.; Spiess, H. W. *Macromolecules* **1996**, *29*, 5427.
(53) Kim, S. H.; Misner, M. J.; Yang, L.; Gang, O.; Ocko, B. M.; Russell, T. P. *Macromolecules* **2006**, *39*, 8473.
(54) Liang, C.; Hong, K.; Guiochon, G. A.; Mays, J. W.; Dai, S. *Angew. Chem., Int. Ed.* **2004**, *43*, 5785.

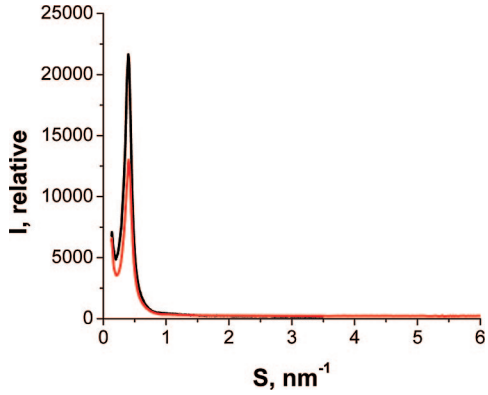

Figure 5. SAXS profiles of the Pl-F108-SiO_2/Al film before (red) and after (black) thermal treatment at 60 °C for 5 h.

samples annealed in the THF atmosphere. Additionally, the structure was not altered when Pl-F108-SiO_2/Al was heated at 80 °C during SAXS measurements directly in the instrument. (This temperature was chosen to compare with the data on variable temperature conductivity; see below.) These data reveal that the structure and ordering of Pl-F108-SiO_2/Al cannot be further improved and are permanently fixed even in the conditions when the precursor block copolymer is fully disordered. We believe that this is due to intermixing and interconnectivity of OIC and triblock copolymer in the composite SPE as indicated by Raman spectroscopy. On the other hand, comparison of the data presented in Tables 1 and 2 clearly shows that degree of ordering does not influence the electrochemical performance of these SPEs.

Here the comparison is due with the improved electrochemical performance described in ref 37 for the composite SPE based on Pluronic F127. We believe that enhanced conductivity of 3.17×10^{-5} S/cm[37] for this sample is due to close to optimal ratio [O]/[Li] = 16. At higher and lower ratios, either there are not enough charge carriers (at low concentration of Li ions) or ordered PEO/Li domains are formed (at high concentration of Li ions) impeding Li ion transport.[55–57] Apparently, the exact optimal concentration of Li ions is specific for each SPE system.[55–57] For the F127-based composite SPEs reported in ref 37, the unfavorable [O]/[Li] ratios also result in disordering of the block copolymer component, allowing one to conclude that ordering is a key factor in the increased conductivity. However, comparing the conductivity of the F127-based SPE reported in ref 37 (3.17×10^{-5} S/cm) with the comparable or higher conductivity values of the F68- and F88-based SPEs reported here (Table 1) suggests that ordering in the block copolymer-based SPEs is not an essential parameter for the improved conductivity while an optimal structure (ratio of the components, intermixing, extended interfaces, etc.) controls the electrochemical performance.

3.6. Variable Temperature Conductivity. In this work we continued our studies to better understand the structure–property relationship for these composite SPEs. Earlier we reported unusual thermal behavior of composite single-ion solid polymer electrolytes.[33] As we illustrate here for Pl-F68-SiO_2/Al as an example, the thermal behavior of SPEs based on block copolymers is similar to that of earlier reported composite SPE. As delivered, the room temperature (23 °C) conductivity for the sample was 4.6×10^{-5} S/cm. When heated (1, red triangles), the conductivity increases fairly rapidly up to 50 °C, and after this the conductivity first levels off and then decreases (Figure 6). If one waits about 5 h at 80 °C (2), the conductivity reaches a new equilibrium. Subsequent cooling from 80 °C to room temperature (3, green circles) causes the conductivity to decrease monotonically, reaching a room temperature value of about 7.5×10^{-6} S/cm (or about a factor of 6 lower than before). Upon cooling immediately below room temperature (4a, green circles) the conductivity continues to drop. If instead the sample is held at 25 °C overnight or longer (4b), the conductivity starts to rise; at some time between about 15 h and 4 days later, it returns to a value close to the original state. From here it can be heated again (5a, blue diamonds) or cooled reversibly (5b, black diamonds). The heating data in Figure 6 were taken after a shorter waiting period at 25 °C, so it was slightly lower than the as-delivered curve.

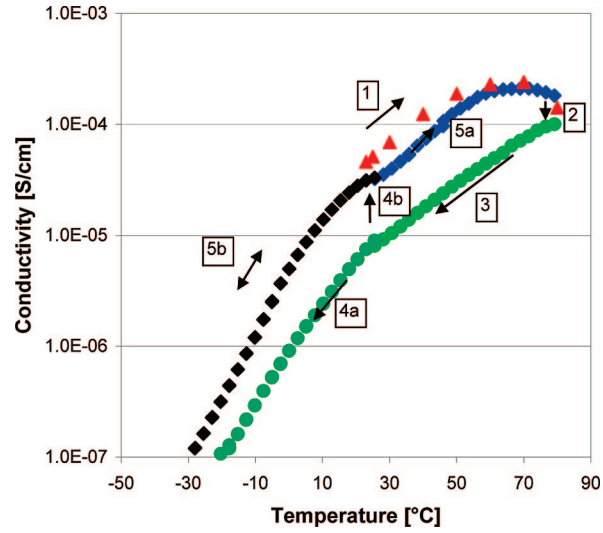

Figure 6. Dependence of conductivity on thermal history of the Pl-F68-SiO_2/Al sample recorded at 50 kHz.

Combining the as-delivered data (up to 50 °C) and the data after supposed recrystallization from −50 to 20 °C, an Arrhenius behavior is approximately applicable with an activation temperature of 7514 K, corresponding to activation energy of 62.5 kJ/mol (Figure 7). This activation energy is only slightly higher than that (~55 kJ/mol) of the composite SPEs reported by us earlier,[29] suggesting no difference in the conductivity mechanism. It is noteworthy that the activation energy reported here is intermediate between those of the composite SPE containing clay particles (11.7 kcal/mol)[58] and of the PEO + Li triflate SPE (108 kJ/mol).[59]

The data obtained (Table 1) show that all the samples based on block copolymers and silicate OIC possess con-

(55) Gray, F. M.; Vincent, C. A.; Kent, M. *J. Polym. Sci., Part B* **1989**, *27*, 2011.
(56) Fu, Y.; Pathmanathan, K.; Stevens, J. R. *J. Chem. Phys.* **1991**, *94*, 6323.
(57) Gupta, S.; Shahi, K.; Binesh, N.; Bhat, S. V. *Solid State Ionics* **1993**, *67*, 97.
(58) Vaia, R. A.; Vasudevan, S.; Krawiec, W.; Scanlon, L. G.; Giannelis, E. P. *Adv. Mater.* **1995**, *7*, 154.
(59) Robitaille, C. D.; Fauteux, D. *J. Electrochem. Soc.* **1986**, *133*, 315.

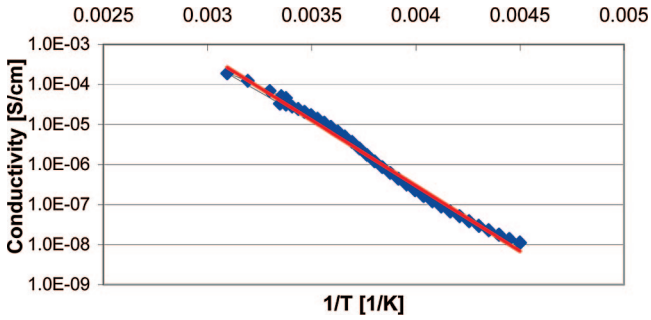

Figure 7. Variable temperature conductivity and Arrhenius plots (red) of the Pl-F68-SiO_2/Al sample.

siderably high conductivities (especially Pl-F68-SiO_2/Al). However, the change of conductivity depending on the thermal history of the sample (Figure 6) seems to be counterintuitive. Indeed, if the change would be determined by melting of the PEO crystallites at 50–60 °C, at 80 °C in fully amorphous SPE the conductivity should increase, not decrease. Further cooling below crystallization temperature (50–60 °C) should result in higher conductivity values than those obtained upon heating, since recrystallization is normally delayed in hybrid SPE. The complex temperature dependence and restoration of higher conductivity value after storage at room temperature suggest that this sample might possess some favorable structure/ordering allowing higher conductivity. At 80 °C this structure is destroyed while after prolonged storage at room temperature it is restored. However, the SAXS measurements carried out at 80 °C show that the structure/ordering remains unchanged under heating. Taking into account these facts and the reasoning in ref 33, we suggest that unusual thermal behavior should be attributed to a composite nature of these SPEs and, in particular, reversible changes of the intermixed OIC and a polymer phase.

3.7. Rheology. Rheological measurements were carried out on two block copolymer-based SPEs: Pl-F68-SiO_2/Al and Pl-F108-SiO_2/Al. For comparison, we also used two SPEs based on 600 MW PEO and the OIC: in one case, the material contained silicate and a similar amount of silicate to that of block copolymer-based samples (designated PEG600-55%-SiO_2/Al),[30] and in the other case, the sample contained a similar amount of alumosilicate OIC (designated PEG600-55%-AlSi).[28] The last two samples were chosen as control and to understand the influence of microphase separation (or ordering for Pl-F108-SiO_2/Al) of a polymeric component (block copolymer vs homopolymer) and of the OIC composition (silica vs aluminosilica).

The results indicate in all cases the elastic modulus is higher than the viscous modulus and frequency independent (see Figure 8); this suggests that the samples are solidlike at room temperature, revealing that in all the materials the OIC components reinforce the polymeric phase (note that L64 is a liquid at room temperature). The material containing Pl-F108-SiO_2/Al showed the highest elastic modulus followed by PEG600-55%-SiO_2/Al, Pl-F68-SiO_2/Al, and PEG600-55%-AlSi which can be attributed to several factors such as the difference in molecular weights, the degree of OIC cross-linking, and the degree of intermixing. The elastic moduli

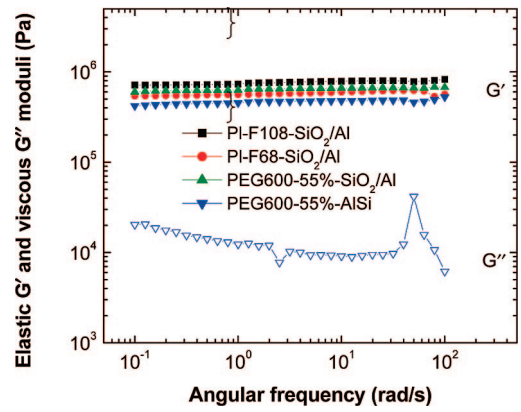

Figure 8. Frequency sweep of the SPEs based on two Pluronics and PEO.

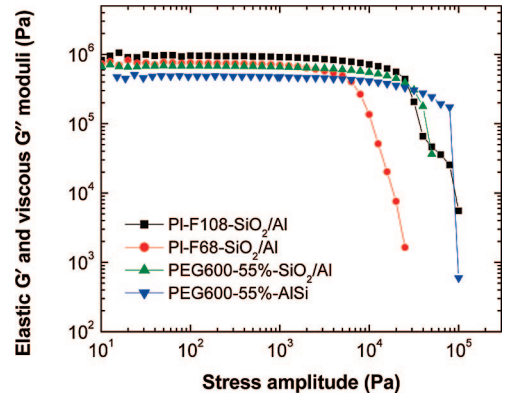

Figure 9. Stress sweep of the SPEs based on two Pluronics and PEO.

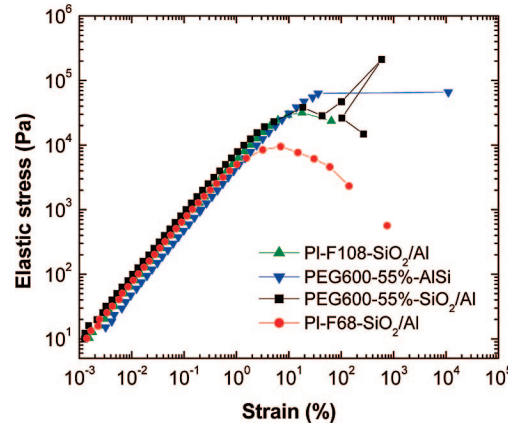

Figure 10. Elastic stress vs strain of the SPEs based on two Pluronics and PEO.

of these materials are comparable to or higher than those of various polymers filled with precipitated silica.[60]

The stress sweeps (Figure 9) show that PEG600-55%-AlSi can be deformed to a larger stress values than the rest of the materials. This is more evident in Figure 10 where the elastic stress is plotted against the strain.[61] This type of plot is useful to determine the yield stress of a material. In this case, the elastic stress plot indicates that PEG600-55%-AlSi has the highest yield stress and the highest yield strain. Pl-F108-

(60) Phewthongin, N.; Saeoui, P.; Sirisinha, C. *J. Appl. Polym. Sci.* **2006**, *100*, 2565.
(61) Walls, H. J.; Caines, S. B.; Sanchez, A. M.; Khan, S. A. *J. Rheol.* **2003**, *47*, 847.

SiO_2/Al and PEG600-55%-SiO_2/Al do not seem to show a big difference in yield stress. We believe that PEG600-55%-AlSi based on aluminosilicate is the strongest because of higher degree of cross-linking in alumosilicate compared to that of silicate in other samples.[30]

Pl-F68-SiO_2/Al shows the lowest yield stress and strain. Note that this material shows the highest conductivity among the SPEs studied; however, currently there are not enough data to support a relationship between the strain–stress properties and electrochemical performance in these particular systems. Remember that conductivities of PEG600-55%-AlSi,[28] Pl-F108-SiO_2/Al, and PEG600-55%-SiO_2/Al are nearly the same, while mechanical properties differ. For PEO/LiTFSI systems,[62] the higher the crystallinity, the higher the modulus of the composite and the lower the ionic conductivity. This is, however, not the case for the materials reported here as PEG600-55%-AlSi[28] and PEG600-55%-SiO_2/Al[30] are fully amorphous, while Pl-F108-SiO_2/Al and Pl-F68-SiO_2/Al have similar and very low degree of crystallinity. Additionally, the presence of the PPO block could have contributed to the increase in elasticity of the material. This effect is only noticeable in PlF108-SiO2/Al because of the lower block copolymer molecular weight of PlF68-SiO2/Al.

Comparison of the stress–strain data on PL-F108-SiO_2/Al and PEG600-55%-SiO_2/Al shows that block copolymer structure/ordering hardly influences the mechanical properties of the material, while the OIC material (better cross-linked alumosilicate vs silicate) has a noticeable influence on mechanical properties.

(62) Li, Y.; Yerian, J. A.; Khan, S. A.; Fedkiw, P. S. *J. Power Sources* **2006**, *161*, 1288.

4. Conclusion

We have demonstrated that composite SPEs based on Pluronics and silicate OIC exhibit enhanced conductivity up to $\sim 5 \times 10^{-5}$ S/cm with improved mechanical properties when compared to pure PEO-based SPEs. Analysis of the Raman spectroscopy data reveals that there is intermixing between polymeric and OIC components in SPEs; the degree of intermixing is dependent on the block copolymer length. The DSC data indicate decreased mobility of the block copolymer component supporting the Raman data on intermixing. Variable temperature conductivity measurements demonstrate unusual thermal behavior of these SPEs which should be attributed to their composite nature or likely to reversible interfacial changes of the mingled OIC and polymer chains. The rheology data indicate that these SPEs are solidlike at room temperature, which suggests that the inorganic phase reinforces the polymeric matrix. The SAXS data clearly demonstrate that block copolymer ordering in the composite SPEs does not lead to enhanced conductivity while the extended interfaces due to intermixing are likely to be responsible for improved electrochemical performance.

Acknowledgment. The authors thank NASA (grant NAG3-2588) and EMBL (grant SAXS-06-29) for financial support of this project.

CM7022218